ISSN 0351–2657
HOBUD7 29(1) 1 (2004)

IS SOLAR PLASMA SINKING DOWN IN VORTICES?

W. PÖTZI[1], P. N. BRANDT[2]

[1] *Observatorium Kanzelhöhe, Universität Graz, A–9521 Treffen, Austria*
[2] *Kiepenheuer-Institut, Schöneckstr. 6, D–79104 Freiburg, Germany*

UDC 523-327-56
Conference paper

Abstract. Three time series of solar granulation filtergrams at different spatial resolutions and of various lengths were investigated for the divergence pattern and its relation to the vorticity at selected scales. The motion vectors for the divergence and vorticity fields were obtained by local correlation techniques. At all resolutions, i.e., granular, mesogranular, and supergranular scales, we find a strong preference of higher vorticity values (of both signs) to be located in regions of negative divergence. That leads to the conclusion that matter sinks down in vortices.

Key words: granulation - mesogranulation - vorticity - divergence

1. Introduction

The H and He II ionization in the solar atmosphere probably are manifest as granulation and supergranulation cells at the solar surface. The regime between these two convection types may be formed by the first ionisation of He at a depth of 7 Mm and is known as the mesogranulation (November et al., 1981). Various techniques had been used to investigate and visualize the mesogranulation — velocity maps with LCT (local correlation tracking) methods (November et. al. 1987, Brandt et al. 1991, Muller et. al. 1992, Roudier et al. 1998), dopplergrams (November et al. 1981, Wang 1989, Deubner 1989), or spectral time series (Straus et al. 1992, Straus and Bonaccini 1997). Brandt et al. (1991) showed that granules of certain types tend to be located preferentially in different mesogranular regions. Pötzi et. al.

(2003) found a correlation between granular types and the divergence pattern - fragmenting and exploding granules were located at positive divergence regions whereas fading granules showed a tendency towards negative divergence; to some extent the actual work is a continuation of this one. Wang et al. (1995) studied Pic du Midi time series and found "that vorticities seem to have a closer association with inflows than outflows". In numerical simulations Zirker (1994) found very strong vortices in intergranular lanes. In theoretical computations of the horizontal divergence-vorticity correlation Rüdiger et al. (1999) found a small but always negative value for the northern hemisphere — with a large scatter, however.

2. The Data

The first data set was observed at the Swedish Vacuum Solar Telescope on La Palma in June 1993 (Simon et al., 1994). The length of the time series is 8.5 hours. It consists of 1500 images, with a time lag of 21 s and spanning an area of 64 to 64 arcsec, corresponding 512 to 512 pixel. The images were taken at 4680 Å using a band pass of 100 Å. Standard image reduction was applied like flat field, dark current correction and derotation. In order to remove seeing and 5 minute oscillations destretching and subsonic filtering were performed before the images were corrected for the telescope point spread function. Most of the images show a rms contrast above 8 %, 175 images are even better than 10 % .

The second data set was observed at the Dutch Open Telescope (DOT), in October 2001 (see also *http://hst33127.phys.uu.nl/~pit/DOT/Showpiece/movies.html*, the movie on AR 9669). The series consists of 198 images taken over a time span of 1 hour and 40 minutes. The center wavelength is 4320 Å and the filter width is 7 Å. The scale of the images is 0.071 arcsec per pixel and their size is 1040 x 864 pixel (= 61 x 74 arcsec). Each image was speckle reconstructed using 100 frames. The complete set was k-Ω filtered for velocities higher than 7 km/s in order to cut off supersonic signals.

The third data set is a time series of 2588 flow fields (FFs) (Shine et al., 2000; Leitzinger et al., 2005). These FFs result from apply-

ing a LCT algorithm to a time series of continuum images, obtained by the SOHO/MDI instrument in January 1997 (original image size: 1024×500 pix, where 1 pix = 0.6 arcsec). After latitude and longitude mapping the finally extracted images, that follow the solar rotation, have a size of 304×480 MDI pixels. For the LCT-algorithm a FWHM of 8 pix was used, while the cell centers were spaced 4 pix apart which yields FFs with a spatial resolution of 4.8 arcsec or 3.5 Mm.

The first data set is located in a quiet region, whereas the other two sets are near active regions. All three data sets are near the solar equator, the first is at N05, the second at N13, and the third spans the latitude range from 05N to 12S.

3. Methods

Divergence and Vorticity: In physical terms, the divergence of a vector field is the extent to which the vector field flow behaves like a source or a sink at a given point. Indeed, an alternative, but logically equivalent definition, gives the divergence as the derivative of the net flow of the vector field across the surface of a small sphere relative to the surface area of the sphere. If the divergence is positive — a source — the matter is coming from somewhere inside the region of interest, in the case of the solar atmosphere the matter must come from lower layers, i.e. matter is flowing upwards. The opposite behaviour holds for a sink.

In simple words, vorticity is the rotation of a vectorfield. A positive vorticity value indicates a counter-clockwise rotation of the vectorfield. For a 2-d velocity field the divergence and the vorticity are defined as:

$$div(\vec{v}) = \nabla\vec{v} = \frac{\partial\vec{v}_x}{\partial x} + \frac{\partial\vec{v}_y}{\partial y} \qquad vort(\vec{v}) = \nabla \times \vec{v} = \frac{\partial\vec{v}_y}{\partial x} - \frac{\partial\vec{v}_x}{\partial y}$$

Visualization The vorticity and the divergence are calculated from each data series at different spatial resolutions, that means that in principle the LCT is performed at different resolutions by applying subwindows of different sizes. E.g. when a subwindow of 8 pixels is

used for the LCT the velocity vectors are smoothed over an area of about 8x8 pixels; due to the LCT method it is not possible to calculate vectors for each individual pixel, because this method compares locations of small subwindows in order to obtain their proper motion. For a distinction between the different regimes of motion, like granulation or mesogranulation, not only the spatial resolution has to be adjusted but also an averaging over a certain time span has to be applied to the divergence and vorticity maps. The granulation has a time scale of about 5 to 10 minutes. If the velocity maps or the divergence are averaged over more than 10 minutes the pattern originating from granular motion begins to be smoothed out. After more than 2 hours almost all of the granular motion is removed, the resulting maps show the behaviour of slower and larger motion regimes — the mesogranulation, and in case of averaging over more than 5 hours the supergranular pattern begins to appear. If the spatial resolution is high and the temporal averaging is long the pattern shows something like mesogranules disturbed by granules.

After the above steps a 2-d histogram is produced with the divergence along the x-axis and the vorticity along the y-axis. In this plot the number of values per histogram bin (which is a rectangle) is coded in grey-scale, otherwise a 3-d plot (surface-plot) would have to be generated. For a better visualization of the relation between the divergence and the vorticity the *mean divergence for a certain vorticity bin* is overplotted (bow-shaped curve). In the following plots only these mean divergence values are displayed. The total ranges for the vorticity and divergence are indicated by the ranges of the axes.

Zero-Test: In order to test and prove the significance of the results, we considered a test. For this purpose we calculated the correlation between vorticity and divergence with rotated data, i.e. the vorticity is rotated against the divergence data by 90, 180, and 270 degrees and then we produced the same plots as above. In such a case the vorticity and the divergence should be uncorrelated and the mean values should therefore be 0, visible in our plots as a straight vertical line at the abscissa ($x = 0$).

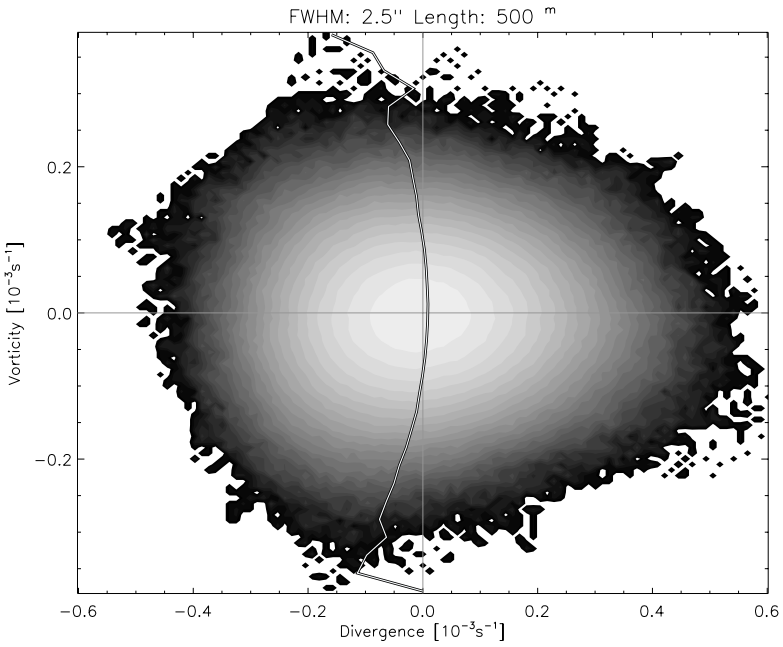

Figure 1: La Palma data at mesogranular scales, the FWHM of the Gaussian window for the LCT was about 20 pixel (2.5 arcsec). The plot shows a 2-d histogram of the divergence and vorticity data. The solid line represents the mean divergence per vorticity bin.

4. Results

The plot in Fig. 1 refers to the full series of the La Palma data. It shows a property, which is more or less the same for all other plots: the divergence distribution is not symmetrical to the vorticity axis. The distribution looks more like an egg than a circle. The peak of the distribution is shifted towards negative divergence values whereas the positive wing is longer than the negative one. This behaviour was noted and discussed earlier by Pötzi et al. (2003); it confirms the findings of Wang et al. (1995). The vorticity is nearly symmetrical around the x-axis for almost all cases. The mean values begin to fluctuate near the highest and lowest vorticity values due to bad statistics.

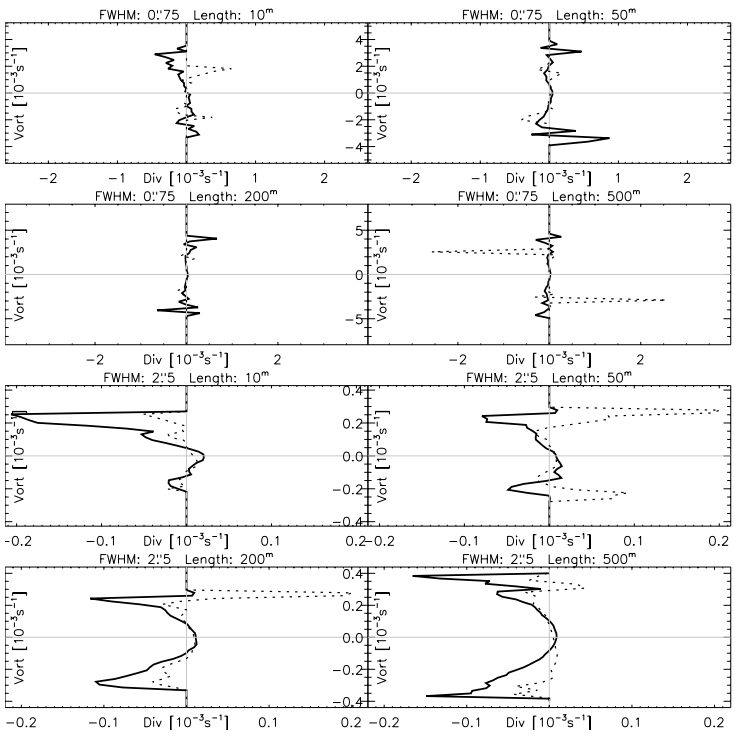

Figure 2: La Palma data at granular and mesogranular scales. The solid line is the mean divergence for a certain vorticity bin, the dotted line represents the results for rotated data sets (see text). The granular data (cf. the top 4 panels) does not show the effect that high vorticty values are located in negative divergence regions, while the mesogranular data (cf. bottom 4 panels) does show the effect.

Granular Scales: For granular scales, i.e. high spatial resolution and short time-averaging, we get results from the La Palma (Fig. 2) and DOT (Fig. 3) data sets. Only these two sets have a spatial resolution that is sufficient for granular velocity vector calculations. In the La Palma set the mean divergence is almost in every case near $x = 0$, there is almost no difference between the normal and the rotated data set. The DOT data very clearly shows deviations of the mean divergence the higher the vorticity is for all plots. In almost every plot the rotated data shows a different behaviour; only for very high vorticity

values strong deviations of the mean divergence from 0 occur, but this is due to bad statistics (scarceness of data) in this range.

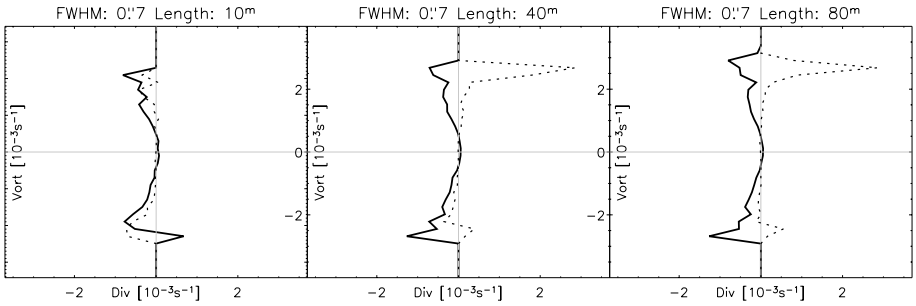

Figure 3: DOT data at granular scales. Also in the intergranular lanes vortices seem to exist.

Mesogranular Scales: At mesogranular scales in the MDI data (Fig. 4) the mean divergence moves towards negative values the higher the vorticity (both positive and negative) values are, but this effect is not very strong. In the La Palma data this effect is much stronger than in the MDI data — the mean divergence is moving definitely towards negative values if the vorticity is higher. For the DOT data we tried to calculate motion vectors at medium resolutions but the data set is too short for good statistics.

5. Discussion

The effect that both positive and negative vortices seem to be located preferentially in regions of negative divergence can be seen at two scales: the granular and the mesogranular scale. In both cases the spatial resolution of the time series is very important. For the granular scales we need images of very high resolution (DOT, 14 pixel per arcsec, speckle reconstruction), if the resolution is lower (La Palma 8 pixel per arcsec, resolution due to seeing approx. 0.3 to 0.5 arcsec) this effect vanishes rapidly. For the mesogranular scales the MDI data set has a resolution which is too low (1.6 pixel per arcsec) and the

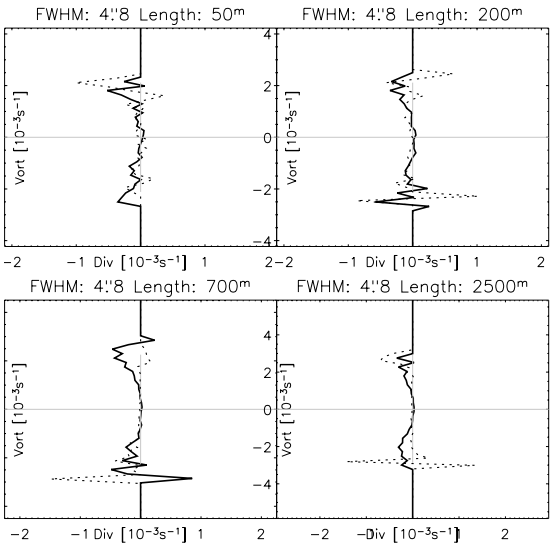

Figure 4: MDI data at mesogranular scales. In the longer time sets (200 and 700 minutes) the effect described above is visible.

La Palma set seems to be just right. This means that the resolution for calculating the velocity vectors has to be well above the scale of interest. It seems that the real granular velocities can be resolved at image scales from about more than 10 pixel per arcsec and for mesogranular velocities the image scale has also to be at some pixel per arcsec. Additionally also the length of the data set has to be taken into account; it should be at least of the time scale of the features that are observed, i.e. several minutes for the granulation and some hours for the mesogranulation.

The deviation of the mean divergence at higher vorticity values means that in inflows the vortices become stronger than in the other regions; in other words, if plasma is sinking down it does so in vortices. This behaviour seems to hold for granulation and mesogranulation - it should also hold for supergranulation. Our results confirm earlier findings by Wang et al. (1995) but contradict the "small, but always negative, divergence-vorticity correlation" found by Rüdiger et al. (1999).

Acknowledgements. We thank R. Shine for supplying the MDI data in pre-reduced form and Martin Leitzinger for help in the interpolation of the data. Pit Sütterlin's support in making the DOT data available is gratefully acknowledged.

References

Brandt, P. N., Ferguson, S., Scharmer, G. B., Shine, R. A, Tarbell, T. D., Title, A. M., and Topka, K.: 1991, *Astron. Astrophys.* **241**, 219.

Deubner, F. L.: 1989, *Astron. Astrophys.* **216**, 259.

Muller, R., Auffret, H., Roudier, Th., Vigneau, J., Simon, G. W., Frank, Z., Shine, R. A., and Title, A. M.: 1992, *Nature* **356**, 322.

Leitzinger, M., Brandt, P. N., Hanslmeier, A., Pötzi, W., and Hirzberger, J.: 2005, Hvar Obs. Bull. **29**, in print.

November, L. J., Toomre, J., Gebbie, K., and Simon, G. W.: 1981, *Astrophys. J.* **245**, L123.

November, L. J., Simon, G. W., Tarbell, T. D., Title, A. M., Ferguson, S. H.: 1987, in G. Athay (ed.) *2nd Workshop on Theoretical Problems in High Resolution Solar Physics*, 121.

November, L. and Simon, G. W.: 1988, *Astrophys. J.* **333**, 427.

Oda, N.: 1984, *Solar Phys.* **93**, 243.

Pötzi, W., Brandt, P. N., Hanslmeier, A.: 2003, *Hvar Obs. Bull.* **27**, 39.

Roudier, Th. and Muller, R.: 1986, *Solar Phys.* **107**, 11.

Roudier, Th., Malherbe, J. M., Vigneau, J., and Pfeiffer, B.: 1998, *Astron. Astrophys.* **330**, 1136.

Rüdiger, G., Brandenburg, A., Pipin, V. V.: 1999, *Astronomische Nachrichten*, **320**, 135.

Simon, G. W., Brandt, P. N., November, L. J., Scharmer, G. B., and Shine, R. A.: 1994, in R. J. Rutten and C. J. Schrijver (eds.), *Solar Surface Magnetism*, 261.

Straus, Th., Deubner, F.-L., and Fleck, B.: 1992, *Astron. Astrophys.* **256**, 652.

Straus, T. and Bonaccini, D.: 1997, *Astron. Astrophys.* **324**, 704.

Wang, H.: 1989, *Solar Phys.* **123**, 21.

Wang, Yi, Noyes, R. W., Tarbell, T. D., Title, A. M.: 1995, *Astrophys. J.*, **447**, 419.

Zirker, J. B.: 1994, *Solar Phys.*, **174**, 47.